The symmetry and polar properties of the ferroelectric phase in BCCD

1997 J. Phys.: Condens. Matter 9 11195

(http://iopscience.iop.org/0953-8984/9/50/020)

J. Phys.: Condens. Matter **9** (1997) 11195–11208. Printed in the UK PII: S0953-8984(97)84611-5

The symmetry and polar properties of the ferroelectric phase in BCCD

L G Vieira†, J L Ribeiro†, A Almeida‡, M R Chaves‡, J Agostinho Moreira‡, A Klöpperpieper§ and J Albers§

† Departamento de Física, Universidade do Minho, P-4709 Braga Codex, Portugal
‡ Departamento de Física, IMAT (núcleo IFIMUP), Faculdade de Ciências da Universidade do Porto, Rua do Campo Alegre 687, 4150 Porto, Portugal
§ Technische Physik, Universität des Saarlandes, D-66200 Saarbrücken, Germany

Received 23 May 1997, in final form 18 September 1997

Abstract. This work reports a study of FIR reflectivity ($\boldsymbol{E} \parallel \boldsymbol{b}$) in betaine calcium chloride dihydrate (BCCD). The spectra are fitted by using the Kurosawa model for the dielectric function. The fits allow the observation of the temperature dependence of the vibrational parameters of the more important polar modes. Particular attention is paid to the lower-frequency polar modes, which are very sensitive to the sequence of phase transitions in this compound. The lower frequencies of the $z(yy)x$-Raman spectrum, measured between room temperature and $T = 20$ K, allow a tentative identification of the symmetry of the low-energy modes that become infrared active at lower temperatures. It is shown that these modes correspond very likely to external modes, where the BCCD molecules behave as rigid units. In the ferroelectric phase, the IR spectrum is compatible with the orthorhombic space group $Pn2_1a$.

The study of the pyroelectric effect along the [100] direction, in a sample cut as a plate parallel to a natural crystalline face to avoid misorientation, does not reveal any trace of an x-component of the spontaneous polarization, previously reported. This result seems to confirm the absence of intrinsic monoclinic distortions in the ferroelectric phase of BCCD.

1. Introduction

Betaine calcium chloride dihydrate (BCCD: $(CH_3)_3N^+CH_2COO^-.CaCl_2.2H_2O$) exhibits a remarkable sequence of phase transitions, from an orthorhombic $Pnma$ phase ($T > 164$ K) to a ferroelectric phase (FE: $T < 47$ K) [1, 2]. Between these two phases, more than fifteen commensurate or incommensurate phases were detected, with a modulation wavevector $\boldsymbol{k} = \delta(T)\boldsymbol{c}^*$ [3–5].

There is a considerable agreement in the literature about most of the main features of the phase sequence in this betaine adduct. However, one can still find some disagreement or less clear aspects in different results reported. For example, the intensities of the Bragg peaks measured in elastic neutron scattering display clear anomalies at several transition temperatures [6, 7], which is at variance with the smooth power law $(T_i - T)^\beta$ suggested by x-ray data [1, 8–10], and, although the existence of a solitonic regime in the first incommensurate phase is strongly supported by EPR [11] or dielectric data [12, 13], there has been no detection of higher satellites in any elastic neutron or x-ray diffractogram.

Another controversial aspect concerns the symmetry and polar properties of the lower-temperature ferroelectric phase. It is well known that first x-ray data reported by Brill and Ehses [1] indicated that the FE phase was modulated ($\delta \approx 1/6$), and that this observation

0953-8984/97/5011195+14$19.50

was confirmed by IR-spectroscopic measurements by Volkov *et al* [14] and Goncharov *et al* [15]. A first indication on the homogeneous (non-modulated) nature of this phase came from EPR [11] and Raman [8] studies, later confirmed by different neutron scattering experiments [5]. There is now a generalized agreement (although not unanimous [16]) on the homogeneous character of the FE phase. However, some questions remain about its symmetry and polar properties. In this paper we focus mainly on this topic.

The first measurements of dielectric hysteresis loops [17] indicated that the spontaneous polarization (P_s) in the FE phase was detected on the (001) plane, with $P_b \gg P_a$. The existence of a small x-component of P_s was also reported from zero-field pyroelectric measurements [18].

The existence of a spontaneous polarization along the [100] direction disagrees with the predictions based on a superspace group approach with a single order parameter $P_y(\boldsymbol{k})$ of Λ_3 symmetry, proposed by Perez-Mato [19], which is very effective in describing the polar nature of the different modulated phases. To account for a possible rotation of the optical indicatrix below $T_i = 164$ K, reported in [20], Dvorak suggested a simultaneous condensation of two order parameters, with the same wavevector [21]. This freezing of two coupled order parameters would give rise to a monoclinic distortion of the average structure of the incommensurate phase and could explain the P_x component of the spontaneous polarization in the FE phase. However, no indication of the monoclinic distortion was obtained by x-ray structural analysis performed at 130 K [22] and at 80 K [23].

The idea of a freezing of a second order parameter at lower temperatures was not however ruled out. In 1992, Almeida *et al* [24] suggested that the anomalous decrease of the intensities of the Bragg satellites observed near 80 K could be due to a triggered freezing of a second order parameter. Also, a detailed analysis of the mode activity in BCCD observed from FIR spectroscopy [25] suggested that the single-order-parameter picture and the orthorhombic symmetry of the commensurate phases was consistent with the spectroscopic data down to about 53 K. However, at lower temperatures, the spectroscopic data for $\boldsymbol{E} \parallel \boldsymbol{b}$ seemed to indicate the existence of monoclinic distortions, reflected by the apparent activity of silent A_u modes and by some ambiguity in the symmetry assignment of the modes observed. For the other polarizations ($\boldsymbol{E} \parallel \boldsymbol{a}$ and $\boldsymbol{E} \parallel \boldsymbol{c}$) the spectroscopic data gave no indications of such distortions and all modes could be assigned to active modes in an orthorhombic ferroelectric phase.

Structural x-ray studies reported by Dernbach [26] and more recently by Ezpeleta *et al* [27] seem to discharge the onset of a monoclinic distortion and ascribe to the FE phase the orthorhombic group $Pn2_1a$. It is therefore of interest to reanalyse the spectroscopic data and the polar properties of BCCD at lower temperatures.

This paper reports new results on the temperature dependence of y-FIR reflectivity, $z(yy)x$-Raman diffusion and x-pyroelectric effect. The undertaken study aims to show the compatibility between the reported symmetry of the FE phase, and the polarization direction and low-frequency spectroscopic data observed in BCCD at low temperatures.

2. Experimental details

Single crystals of BCCD were grown from aqueous solution and cut into oriented platelets of about $10 \times 10 \times 2$ mm^3 for infrared, $3 \times 3 \times 3$ mm^3 for Raman and $5 \times 10 \times 1$ mm^3 for pyroelectric measurements.

The infrared reflectivity measurements were performed in the spectral range 20–4000 cm^{-1} with a Bruker IFS 66V FTIR spectrometer. The spectra were obtained in quasi-normal incidence using a combination of sources (Hg arc and globar lamps), detectors

(DTGS with KBr or polyethylene windows and Si bolometer) and beam-splitters (KBr and Mylar of several thicknesses). An aluminium mirror was used as reference. The resolution was better than 2 or 4 cm^{-1}, respectively for the 20–400 cm^{-1} and 400–4000 cm^{-1} spectral ranges.

Low temperatures were obtained by using an Oxford continuous flow cryostat, with KBr or polyethylene windows. The infrared reflectivity was measured only on cooling (cooling rates were smaller than -0.5 K min^{-1}). The spectra were registered at constant temperature, after a waiting time of the order of 20 minutes to achieve a good thermal equilibrium. The temperature stability was better then 0.1 K. Special care was taken in mounting the sample to avoid thermal strain of the sample.

The $z(yy)x$-Raman spectra were obtained with a Jobin–Yvon T64000 spectrometer, equipped with a CCD detector. A 200 mW line of an argon laser (514.5 nm) was used. The resolution achieved was of the order of 2 cm^{-1}. The samples were placed in a closed cycle helium cryostat, with temperature stability of about 0.5 K in the range 12 K–300 K. To obtain a good temperature stability and homogeneity, a copper mask was used to enclose the sample. The spectra were registered at constant temperature after a waiting time of about 15 minutes.

The pyroelectric effect was measured along the $\boldsymbol{a}$-axis using a short-circuit technique previously described [28]. In order to avoid misorientations of the sample, we have used a plate ($5 \times 3 \times 1$ mm^3) with a (100) natural face and took particular care in achieving a good parallelism of the other face. All measurements were made under a d.c. electric field of 100 V cm^{-1} in order to avoid the formation of domains in the phases polar along this direction ($\delta = 1/4$ and $\delta = 1/6$), as spurious charges can be pinned at the domain walls. The electrical polarization was obtained by integration of the pyroelectric current. The technique allows the detection of a change of the polarization as low as 0.5 nC cm^{-2}.

3. Results and discussion

The study previously reported by Kamba *et al* [25] clearly shows that the infrared spectra for $\boldsymbol{E} \parallel \boldsymbol{b}$ are very sensitive to the sequence of phase transitions in BCCD. We focused our attention on the reflectivity spectra for this polarization $R_b(\omega, T)$ in the frequency range between 20 and 4000 cm^{-1}. Above 500 cm^{-1}, all modes detected correspond to internal modes of betaine and H_2O. The more intense among these modes correspond to H_2O (3350 cm^{-1}), CH_3 (ν_a: 2950 cm^{-1}) and COO^- (ν_a: 920 cm^{-1} and π: 530 cm^{-1}). We will be mainly interested in the low-frequency external modes of BCCD.

Figure 1 shows $R_b(\omega, T)$ for temperatures between 20 and 290 K and frequencies in the range 20–600 cm^{-1}. As can be seen, the shape of the spectra reflects the sequence of phase transitions. In order to analyse the temperature dependence of $R_b(\omega, T)$ we fitted the spectra using the Kurosawa model [29] for the dielectric function, which has been shown to be well adapted to materials where active modes exhibit damping functions strongly dependent on frequency or/and very different TO and LO frequencies:

$$\varepsilon(\omega) = \varepsilon_\infty \prod_j \frac{\Omega_{jlo}^2 - \omega^2 - \mathrm{i}\omega\gamma_{jlo}}{\Omega_{jto}^2 - \omega^2 - \mathrm{i}\omega\gamma_{jto}}. \tag{1}$$

The fit allows us to follow the temperature dependence of the parameters characterizing each relevant mode (Ω_{to}, dielectric strength and γ_{lo} and γ_{to} damping constants).

Figure 2(a) displays the temperature dependence of the imaginary part of the dielectric function $\varepsilon_2(\omega, T)$ deduced from the fit. Each peak in $\varepsilon_2(\omega, T)$ corresponds to the frequency

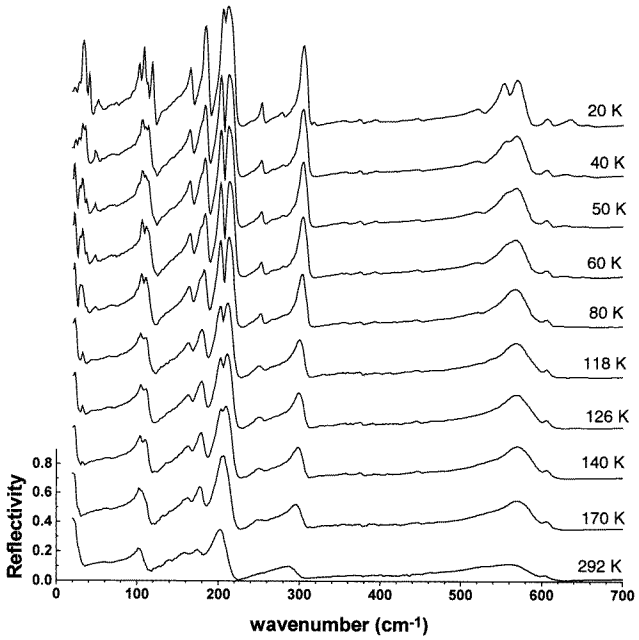

Figure 1. Far-infrared reflectivity of BCCD for $\boldsymbol{E} \parallel \boldsymbol{b}$ ($20\ \mathrm{cm}^{-1} < \omega < 700\ \mathrm{cm}^{-1}$) at different temperatures ($20\ \mathrm{K} < T < 292\ \mathrm{K}$).

of an active TO mode. The plot of the lower frequencies Ω_{to} ($n < 140\ \mathrm{cm}^{-1}$) versus the temperature (figure 2(b)) illustrates clearly the sensitivity of the spectra to the main phase transitions: as the temperature is lowered, several modes are activated or extinguished, and the temperature dependence of some frequencies displays clear anomalies at the main phase transitions (*Pnma*–IC–2/7–IC–1/4–1/5–1/6–FE). Figure 2(b) displays the temperature dependence of the lower-energy TO modes.

In order to understand the temperature induced modifications of the spectra, we shall first analyse the characteristics of $R_b(\omega, T)$ measured in the PE and FE non-modulated phases. Figure 3 shows in more detail $R_b(\omega)$ and $\varepsilon_2(\omega, T)$ measured at 292 K (PE phase) and at 20 K (FE phase), in the frequency region $20\ \mathrm{cm}^{-1} < \nu < 350\ \mathrm{cm}^{-1}$. As can be seen, the spectrum at room temperature displays three modes with $\Omega_1 < 20\ \mathrm{cm}^{-1}$, $\Omega_5 = 65\ \mathrm{cm}^{-1}$ and $\Omega_8 = 109\ \mathrm{cm}^{-1}$. In the FE phase additional modes arise due to the loss of symmetry elements.

The frequency of the mode Ω_1 could not be accurately measured between room temperature and $T_1 = 164$ K. In [25] it is shown, from the analysis of the transmission spectra measured with a quasi-optic Epsilon spectrometer based on a backward-wave oscillator, that the frequency of this mode is of about $15\ \mathrm{cm}^{-1}$ at room temperature. Below $T_1 = 164$ K, the frequency of the mode increases well above $20\ \mathrm{cm}^{-1}$, allowing its accurate detection with our spectrometer.

From the knowledge of the *Pnma* structure, one can deduce that among the 336 lattice modes there are 37 optical B_{2u} modes, IR active for the polarization considered. The lower-frequency modes must correspond to the external modes involving the four BCCD molecules of the unit cell as rigid structures. Factor group and site symmetry analysis indicate that the symmetry of these modes is that described in table 1 (the coordination number for the *Pnma* phase is $Z = 4$).

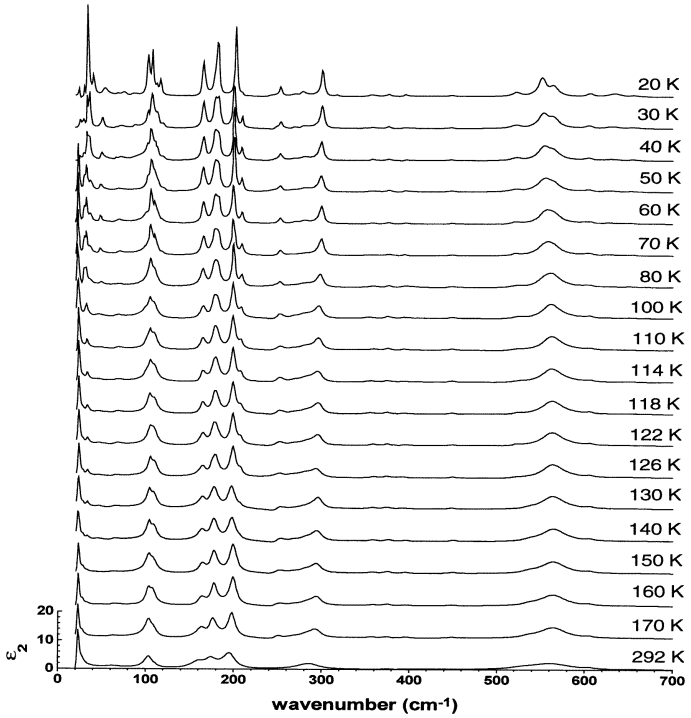

(a)

Figure 2. (a) Imaginary part of the dielectric function (ε_2) in the frequency range 20 cm^{-1} < ω < 700 cm^{-1} for different temperatures. This function was calculated from the fit of the spectra to the Kurosawa function for $\varepsilon_1 + i\varepsilon_2$. (b) Temperature dependence of the TO frequencies of the lower-energy polar modes in BCCD. The range of stability of the more stable phases is shown at the bottom of the figure. Below 80 cm^{-1}, the two B_{2u} librational modes observed in the *Pnma* phase split into five modes ($2B_{2u} + 3A_g$) as expected for a transition to a ferroelectric $Pn2_1a$ phase.

Table 1. External modes in BCCD and their symmetry.

IR	Acoustic	Translat. Optic	Librational	Symmetry
A_g	—	2	1	$xx; yy; zz$
B_{2u}	1	—	2	y
A_u	—	1	2	—
B_{2g}	—	2	1	xz
B_{1u}	1	1	1	z
B_{3g}	—	1	2	yz
B_{1g}	—	1	2	xy
B_{3u}	1	1	1	x

As can be observed, there are only two low-frequency B_{2u} betaine-$CaCl_2.2H_2O$ librational modes. These modes can be tentatively related to the lower-frequency modes detected in $R_b(\omega)$ ($\Omega_1 < 20$ cm^{-1}, $\Omega_5 = 65$ cm^{-1}).

In an orthorhombic $Pn2_1a$ ferroelectric phase, the A_g modes, $z(yy)x$-Raman active in the PE phase, become infrared active (A_1 symmetry) in the $\boldsymbol{E} \parallel \boldsymbol{b}$-polarization.

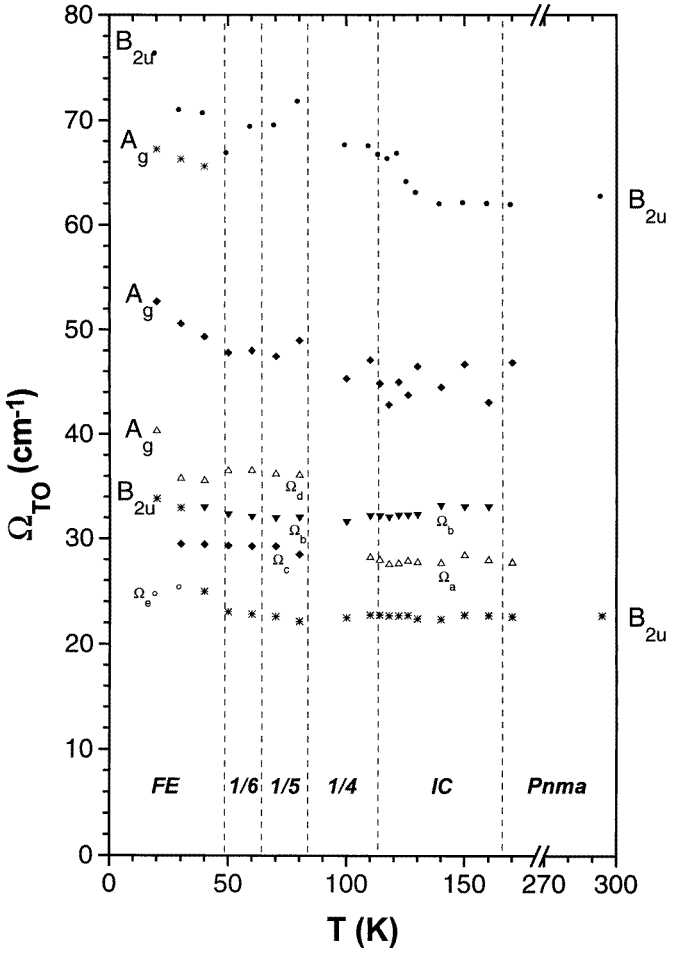

(b)

Figure 2. (Continued)

One should therefore expect the appearance of these modes in the $R_b(\omega)$ spectrum. On the other hand, if the FE phase has a monoclinic symmetry, one must consider two possibilities, depending on the point group symmetry (C_2 or C_S). In the first case (space group $P12_11$), one should expect also the activation of the modes A_u and B_{2g}. In the second case (space group P_{11a}), the additional modes becoming IR active would correspond to the symmetries B_{1g} and B_{3u}. According to table 1, this would give rise to a possible detection of eleven or ten low-frequency external modes ($\Omega \approx 80$ cm^{-1}) in the FIR reflectivity spectrum of the FE phase. As can be seen in more detail in figure 3 this is not observed experimentally.

In order to confirm the consistency of the IR data with the orthorhombic nature of the lower-temperature phase we studied the temperature dependence of the $z(yy)x$-Raman spectra of BCCD, between the PE and FE phases (see figure 4). At room temperature, and below 100 cm^{-1}, we detect three modes with frequencies $\Omega_2 = 33$ cm^{-1}, $\Omega_3 = 49$ cm^{-1}, $\Omega_4 = 60$ cm^{-1} (the next mode is detected at $\Omega = 97$ cm^{-1}). As before, we ascribe to these three lower-energy modes to the three A_g external modes of table 1.

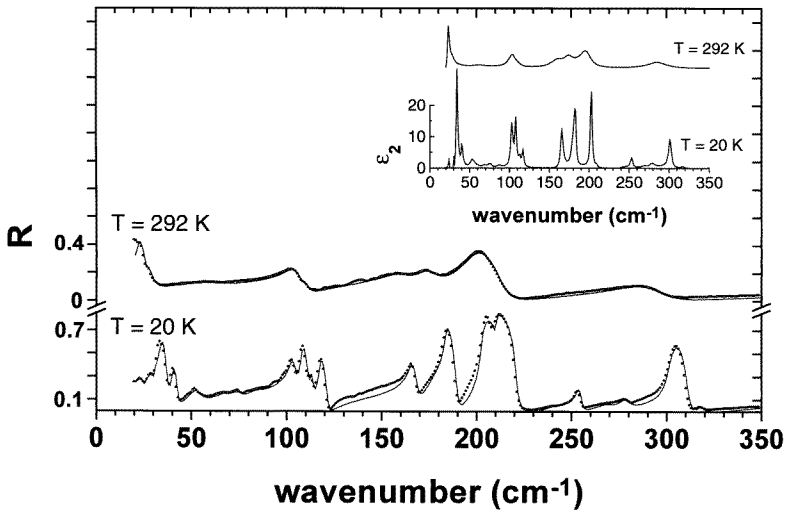

Figure 3. Detail of the FIR reflectivity for $\boldsymbol{E} \parallel \boldsymbol{b}$ at room temperature and at 20 K: the circles represent the experimental points and the line represents the fit to the Kurosawa function. Note that all the details of the experimental spectrum taken at 20 K are very accurately described by the fit below 120 cm^{-1}.

The inset of the figure shows the imaginary part of the dielectric function corresponding to the two spectra shown.

Table 2. Lower $A_g + B_{2u}$ energy modes observed at room temperature and at 20 K.

	290 K		20 K		
Pnma	IR	Raman	IR	Raman	$Pn2_1a$
	—	—	25 cm^{-1}		i
	—	—	30 cm^{-1}		i
B_{2u}	< 20 cm^{-1}		34 cm^{-1}	36 cm^{-1}	A1
A_g		33 cm^{-1}	40 cm^{-1}	43 cm^{-1}	A1
A_g		49 cm^{-1}	53 cm^{-1}	59 cm^{-1}	A1
A_g		60 cm^{-1}	67 cm^{-1}	63 cm^{-1}	A1
B_{2u}	63 cm^{-1}		76 cm^{-1}	71 cm^{-1}	A1

As the temperature is lowered, the frequencies of the A_g modes are shifted towards higher values and other modes are activated. At $T = 20$ K, and below 80 cm^{-1}, the $z(yy)x$-Raman spectrum shows five clear modes with frequencies $\Omega_1 = 36$ cm^{-1}, $\Omega_2 = 43$ cm^{-1}, $\Omega_3 = 59$ cm^{-1}, $\Omega_4 = 63$ cm^{-1} and $\Omega_5 = 71$ cm^{-1}. From the temperature dependence of the mode frequencies, we can relate the modes Ω_2, Ω_3, Ω_4 to the three A_g modes detected in the PE phase.

Table 2 lists the lower frequency modes detected at room temperature and at $T = 20$ K in $R_b(\omega)$ and in the $z(yy)x$-Raman spectra.

With the exception of the weak modes observed at 25 cm^{-1} and 30 cm^{-1} there is a clear correspondence between the two sets of modes. It is apparent that, at 20 K, we detect the same five modes by Raman and by IR reflectivity, in agreement with the fact that the *Pnma* modes A_g and B_{2u} become simultaneously IR and Raman active, due to the loss of the [010] mirror plane ($Pnma \rightarrow Pn2_1a$ phase transition). We further stress that, at

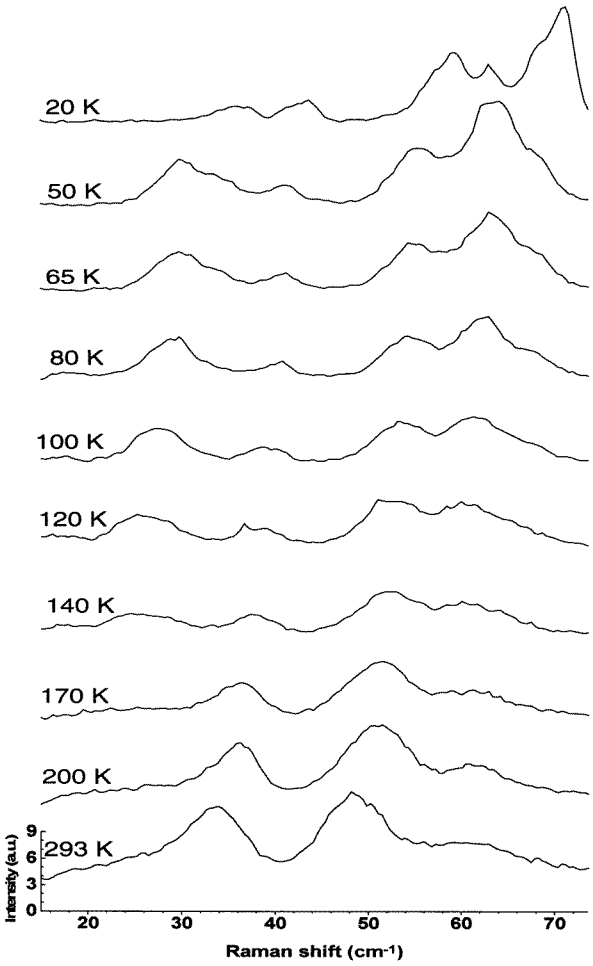

Figure 4. Low-energy $z(yy)x$-Raman spectrum at room temperature. The three modes observed below 60 cm^{-1} correspond very likely to the three external librational A_g modes expected for the *Pnma* phase.

variance with the analysis reported in [25], we do not ascribe to any mode detected above 30 cm^{-1} a symmetry A_u. Moreover, our mode assignment is quite consistent with the expected number of active low-energy external modes listed in table 1.

In order to discuss the possible origin of the additional weak modes detected below 30 cm^{-1} and to confirm the correspondence suggested in table 2, one needs to analyse the modifications observed on the spectra along the temperature range of stability of the different modulated phases. A first observation concerns the fact that these modes are not detected in the Raman spectra. This suggests that they may correspond to the metastable persistence of modulated domains, enhanced by surface defects, as only a thin layer of the sample contributes to the IR spectra in this frequency range. In fact, for $T = 30$ K and $\omega = 30$ cm^{-1}, the penetration length obtained from the data is of the order of 0.08 mm.

As shown in figure 2(b), the onset of the incommensurate phase at $T_1 = 164$ K is

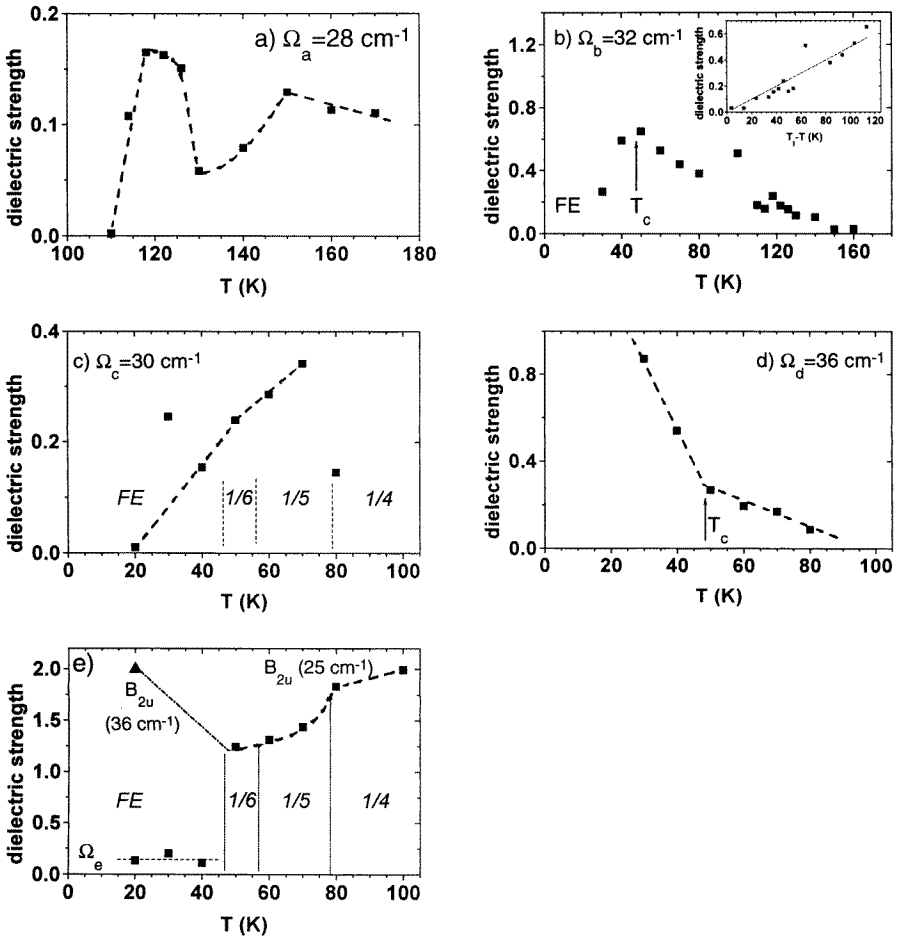

Figure 5. Temperature dependence of the dielectric strength of the lower-energy modes observed in the temperature range of stability of the modulated phases. The different modes identified by a frequency Ω_i ($i = a, b, c, d$ and e) correspond to those shown in figure 2(b).

marked by the rise of two additional weak modes with frequencies $\Omega_a \approx 28$ cm^{-1} and $\Omega_b = 32$ cm^{-1}. As can be seen in figure 5(a), the dielectric strength of the mode Ω_a increases as the temperature is lowered in the first IC phase, decreases in the vicinity of the $\delta = 2/7$ phase, rises again in the second IC phase and vanishes as the system enters the $\delta = 1/4$ phase. Quite differently, the dielectric strength of the mode $\Omega_b \approx 32$ cm^{-1} rises as the temperature decreases down to 50 K and drops down sharply as the system approaches the FE phase. This mode could not be detected in the spectra taken at 20 K.

In a modulated phase with a modulation wavevector $\boldsymbol{k}(T)$, several modes with $\boldsymbol{q} = \pm n\boldsymbol{k}$ may become active. The dielectric strength of a $\boldsymbol{q} = \pm n\boldsymbol{k}$ mode is expected to be proportional to ρ^{2n}, ρ being the amplitude of the modulation wave (the order parameter). The activation of these modes is due to the folding of the Brillouin zone and is therefore independent of the particular value of $\boldsymbol{k}$: they may be detected in an incommensurate as well as in a commensurate phase. The behaviour displayed by the dielectric strength of the

mode Ω_b (see figure 5(b)) seems compatible with such an origin. Moreover, and as shown in the inset of figure 5(b), the dielectric strength of this mode follows reasonably, just below $T_1 = 164$ K, a linear dependence on $(T_1 - T)$, as expected for the IR active component of the doublet $\pm\boldsymbol{k}$.

As referred to above, the mode Ω_a is not detectable in the phase $\delta = 1/4$ and its strength displays a minimum in the vicinity of the $\delta = 2/7$ phase. It is possible that this mode might correspond to the activation of the lower-frequency A_g mode as a result of a local loss of the mirror plane perpendicular to $\boldsymbol{b}$, also observed by EPR [11] in this temperature region. The absence of activity of this mode in the phase $\delta = 1/4$ would correspond then to the reappearance of this symmetry element in the unit cell of this commensurate phase.

In the temperature range of stability of the phases $\delta = 1/5$ and $\delta = 1/6$, and in a frequency range below 40 cm^{-1}, we observe the low-frequency B_{2u} and the Ω_b modes as well as two additional modes with frequencies $\Omega_c \approx 30$ cm^{-1} and $\Omega_d \approx 37$ cm^{-1}. The strengths of these two additional modes behave differently as the system enters the FE phase (see figures 5(c) and (d)): the intensity of the mode Ω_d increases in the FE phase while that corresponding to the mode Ω_c decreases strongly below 50 K and is undetectable at 20 K. As before, one can assume that the mode Ω_d correspond to the activation of a Γ-mode, while the mode Ω_c may correspond to a $\boldsymbol{q} \neq 0$ mode, possibly of higher order ($\boldsymbol{q} = 2\boldsymbol{k}$ (?)).

According to the single-parameter model for BCCD, in all the possible space groups for the $\delta = 1/5$ phase ($P2_12_12_1$; $P112_1/n$ or $P112_1$) the mirror [010] is lost, thus resulting once again a possible activation of the modes A_g. We therefore ascribe this symmetry to the mode Ω_d.

In the FE phase, the two weak modes that were not identified as active modes of the orthorhombic $Pn2_1a$ have frequencies corresponding to those of the lower B_{2u} and of the Ω_c modes in the modulated phases $\delta = 1/5$ and $\delta = 1/6$. As shown in figure 5(e), the strength of the lower-energy B_{2u} mode, as well as its frequency (see figure 2(b)), increases sharply on entering the FE phase. However, one can still detect at 20 K a weak Ω_e mode, with a frequency corresponding to that of the B_{2u} mode in the modulated phases. We therefore believe that the two lower-energy modes detected in the spectra reflect the persistence of metastable inhomogeneities (modulated domains) in the ferroelectric phase.

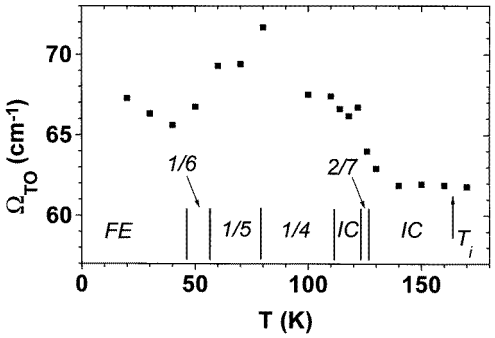

Figure 6. The TO frequency of the B_{2u} mode observed at room temperature at about 65 cm^{-1} displays clear anomalies at the transition temperatures between the more stable phases in BCCD.

To conclude the analysis of the IR data, we would like to stress further the sensitivity of $R_b(\omega, T)$ to the phase sequence in BCCD. Figure 6 displays the temperature dependence of Ω_{to} of the B_{2u} mode observed at about 60 cm^{-1}. As can be seen, the temperature dependence

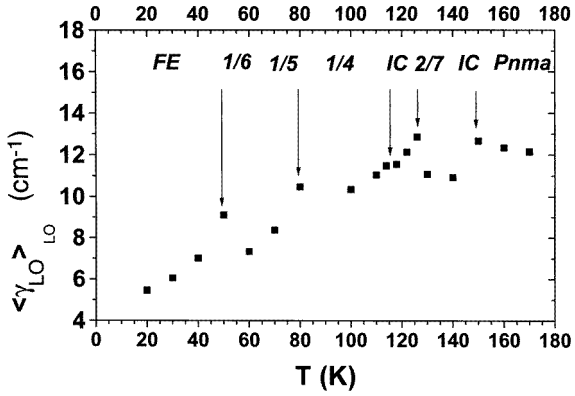

Figure 7. The weighted damping constant calculated for all modes according to equation (3), displays clear anomalies at the different transition temperatures.

of the frequency of this mode shows clear anomalies at the transition temperatures between the more stable phases (*Pnma*–IC–2/7–IC–1/4–1/5–1/6–FE). Moreover, the fit of the spectra allows us to look for other marks of the phase sequence. Figure 7 shows the temperature dependence of an effective damping constant, calculated over all frequencies measured as:

$$\langle\gamma_{lo}\rangle_{lo} = \left(\sum_j \gamma_{jlo}\,\Delta\varepsilon_{jlo}\right)\left(\sum_j \Delta\varepsilon_{jlo}\right)^{-1} \tag{2}$$

where γ_{jlo} represents the longitudinal damping constant of the jth mode with a longitudinal strength $\Delta\varepsilon_{jlo}$:

$$\Delta\varepsilon_{jlo} = \varepsilon_\infty^{-1}\Omega_{jlo}^{-2}\prod_k(\Omega_{kto}^2 - \Omega_{jlo}^2)\left(\prod_{k\neq j}(\Omega_{klo}^2 - \Omega_{jlo}^2)\right)^{-1}. \tag{3}$$

This effective damping constant is expected to reflect the relative weight of anharmonic effects and to display anomalies at a critical point. As can be seen this is observed experimentally.

Let us focus now on the polar properties of the ferroelectric phase in BCCD. As mentioned above, the proposed symmetry ($Pn2_1a$) contradicts the previous results concerning the measurements of the spontaneous polarization along $\boldsymbol{a}$, which provided evidence for a small polarization of the order of 5 nC cm^{-2} along this direction. In fact, this polarization could indicate a monoclinic symmetry P_{11a}.

As the polarization along the $\boldsymbol{b}$-axis is of the order of 1 μC cm^{-2}, a misorientation of the sample as small as 0.2 degrees could originate an erroneous value of the polarization detected along $\boldsymbol{a}$. For this reason, we paid particular attention to orientation of the sample, that was cut along a plane parallel to a (100) natural face.

Figures 8(a) and (b) show the pyroelectric current $I_a(T)$ versus the temperature obtained both on heating and cooling runs. The curves of electrical polarization calculated from the data are also depicted in the same figures. As it was previously reported, the commensurate phases $\delta = 1/4$ and $\delta = 1/6$ exhibit a clear polarization along the $\boldsymbol{a}$-axis. However, in the range of stability of the homogeneous ferroelectric phase, we could not detect any polarization along this direction. This means that this polarization, if exists, must be smaller

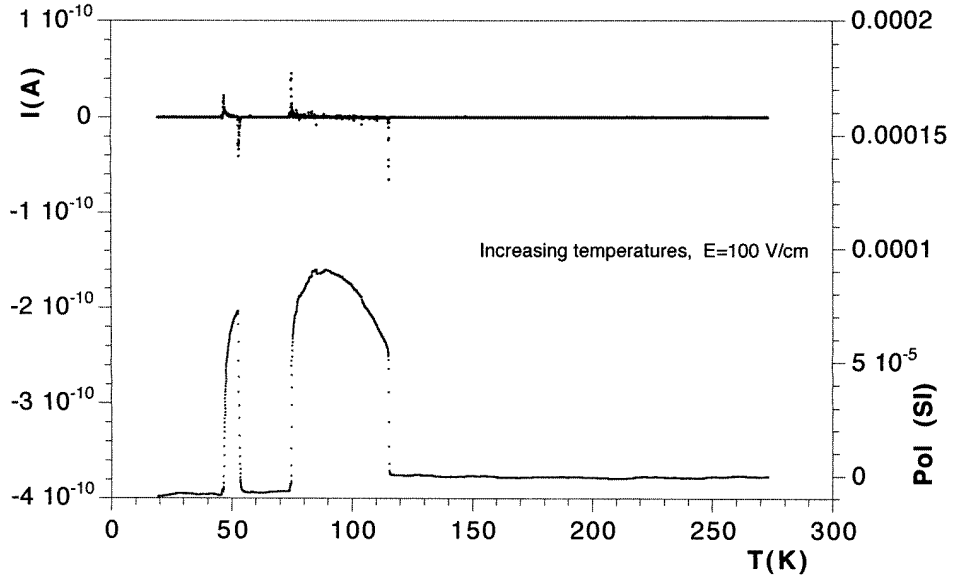

(a)

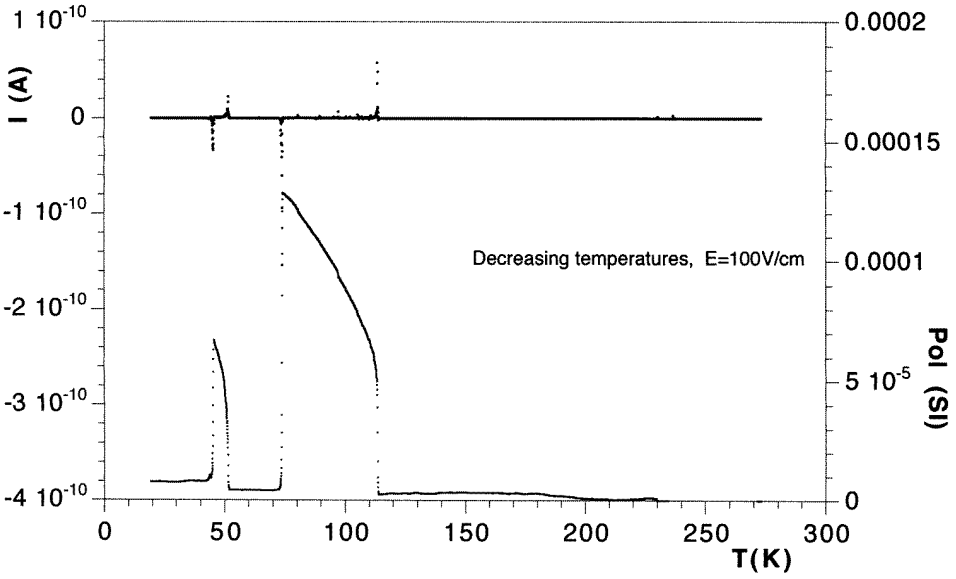

(b)

Figure 8. Pyroelectric current and electrical polarization measured along [100] on heating (a) and on cooling (b) runs. Even under a bias field of 100 V cm^{-1} there is no evidence for an a-component of the spontaneous polarization in the FE phase. The polar phases shown correspond to the commensurate phases $\delta = 1/4$ (115 K $> T >$ 78 K) and $\delta = 1/6$ (56 K $> T >$ 47 K).

than 0.5 nC cm^{-2}, and that the monoclinic distortions that originate such a polarization are extremely small or inexistent.

4. Conclusions

The results of FIR reflectivity, Raman diffusion and pyroelectric effect reported in this work are consistent with the symmetry breaking expected from the single-order-parameter picture proposed by Perez-Mato for the phase transition sequence of BCCD.

The conjugated analysis of the reflectivity and Raman data allowed a symmetry assignment to the lower-energy modes observed in the ferroelectric phase. The number and the symmetry of the modes detected between 30 cm^{-1} and 80 cm^{-1} are consistent with a symmetry $Pn2_1a$ of the ferroelectric phase, recently reported from x-ray studies.

Two weak modes, detected in the reflectivity data below 30 cm^{-1}, were not ascribed to Γ-point modes. In fact, the analysis of the temperature dependence of the frequency and dielectric strengths of these modes along the phase transition sequence suggest that these modes may reflect rather a metastable persistence of modulated domains, specially at the surface of the sample, than a onset of additional distortions giving rise to a monoclinic symmetry. Moreover, if these modes were activated A_u and B_{2g} or B_{1g} and B_{3u} modes, one should expect their detection also in the $z(yy)x$-Raman spectrum, which is not observed experimentally.

Pyroelectric data give no evidence for a P_a component of the spontaneous electric polarization, contrary to previously reported results. This gives further support to the conclusions drawn from the analysis of the spectroscopic data and clearly excludes the possibility of a C_S point group symmetry for the ferroelectric phase of BCCD.

Acknowledgments

The authors are indebted to Professor F Gervais (CNRS—Orléans) for many fruitful discussions and remarks. They also thank M Costa for his technical assistance. This work was partially supported by Junta Nacional de Investigaçad Cientifica e Technológica, Projecto Praxis XX1/2/2.1/FIS/26/94 and by Centro de Fisica da Universidade do Porto.

References

[1] Brill W and Ehses K H 1985 *Japan. J. Appl. Phys.* **24** (Supplement 2) 826
[2] Brill W, Schildkamp W and Spilker J 1985 *Z. Kristallogr.* **172** 281
[3] Ribeiro J L, Chaves M R, Almeida A, Albers J, Klöpperpieper A and Müser H E 1989 *Phys. Rev.* B **39** 12 320
[4] Unruh H G, Hero F and Dvorák V 1989 *Solid State Commun.* **70** 403
[5] Chaves M R, Kiat J M, Schwarz W, Schneck J, Almeida A, Klöpperpieper A and Müser H E 1993 *Phys. Rev.* B **48** 5852
[6] Chaves M R, Almeida A, Tolédano J, Schneck J, Kiat J M, Schwarz W, Ribeiro J L, Klöpperpieper A and Albers J 1993 *Phys. Rev.* B **48** 13 318
[7] Chaves M R, Almeida A, Kiat J M, Tolédano J, Schneck J, Glass R, Schwarz W, Ribeiro J L, Klöpperpieper A and Albers J 1985 *Phys. Status Solidi* b **189** 97
[8] Ao R and Schaack G 1988 *Ferroelectrics* **80** 105
[9] Etxbarria J, Perez-Mato J M, Breczewski T and Arnaiz A R 1990 *Solid State Commun.* **76** 461
[10] Wilhelm H and Unruh H G 1991 *Z. Kristallogr.* **195** 75
[11] Ribeiro J L, Fayet J C, Emery J, Pézeril M, Albers A, Klöpperpieper A, Chaves M R and Almeida A 1988 *J. Physique* **49** 813

[12] Ribeiro J L, Chaves M R, Almeida A, Albers A, Klöpperpieper A and Müser A 1989 *J. Phys.: Condens. Matter* **1** 8011
[13] Freitag O 1992 *PhD Thesis* Universität des Saarlandes
[14] Volkov A, Goncharov A, Yu G, Kozlov G, Albers A and Petzelt J 1996 *Pis. Zh Eksp. Teor. Fiz.* **44** 469
[15] Goncharov Y, Kozlov G, Volkov A, Albers A and Petzelt J 1988 *Ferroelectrics* **80** 221
[16] Wabra N *Seminar 'Inkommensurable Strukturen' (Ehbenhausen, 1995)* reports the observation of a modulation $= 1/6$ at low temperatures
[17] Rother H J, Albers J and Klöpperpieper A 1984 *Ferroelectrics* **54** 107
[18] Ribeiro J L, Chaves M R, Almeida A, Albers J, Klöpperpieper A and Müser H E 1988 *Ferroelectr. Lett.* **8** 135
[19] Perez-Mato J M 1988 *Solid State Commun.* **67** 1145
[20] Kroupa J, Albers J and Ivanov N 1990 *Ferroelectrics* **105** 345
[21] Dvorak A 1990 *Ferroelectrics* **104** 135
[22] Zúniga F, Ezpeleta J, Perez-Mato J M, Paciorek W and Madriaga G 1991 *Phase Transitions* **31** 29
[23] Ezpeleta J M, Zúniga F, Perez-Mato J M, Paciorek W and Breczewski T 1992 *Acta. Crystallogr.* B **48** 261
[24] Almeida A, Chaves M R, Kiat J, Schneck J, Schwarz W, Tolédano J C, Ribeiro J L, Klöpperpieper A, Müser H E and Albers J 1992 *Phys. Rev.* B **45** 9576
[25] Kamba S, Dvorák V, Petzelt J, Goncharov Y, Volkov A and Kozlov G 1993 *J. Phys.: Condens. Matter* **5** 4401
[26] Dernbach D 1993 *PhD Thesis* Universität des Saarlandes
[27] Ezpeleta J M, Zuniga F, Paulus W, Cousson A, Hlinka J and Quilichini M 1996 *Acta Crystallogr.* B **52** 810
[28] Chaves M R, Amaral M H and Ziolkiewicz S 1980 *J. Physique* **41** 259
[29] Kurosawa T 1963 *J. Phys. Soc. Japan* **16** 1298